

Published in IET Control Theory and Applications
 Received on 23rd May 2009
 Revised on 8th January 2010
 doi: 10.1049/iet-cta.2009.0249



Theory and experiments of global adaptive output feedback tracking control of manipulators

*J. Moreno-Valenzuela*¹ *V. Santibáñez*² *E. Orozco-Manríquez*¹
*L. González-Hernández*¹

¹Centro de Investigación y Desarrollo de Tecnología Digital del IPN CITEDI-IPN, Ave. del Parque 1310, Mesa de Otay, Tijuana, B.C., 22510, Mexico

²Instituto Tecnológico de La Laguna, Blvd. Revolución y Cuauhtémoc, Torreón, Coah., 27000, Mexico
 E-mail: moreno@citedi.mx

Abstract: A new adaptive controller for robot manipulators is proposed. The new approach uses only position measurements. The main conclusions derived from the closed-loop system analysis are in two main results. In the first one, the global convergence of the position and velocity tracking errors is stated by using a condition that relates the viscous friction damping and the desired joint speed. In the second one, such a condition is dropped out but the local exponential stability of the closed-loop system is shown. To confirm the theoretical conclusions, a detailed experimental study in a two degrees-of-freedom direct-drive manipulator is provided, where the performance of the new controller is compared with respect to a known output feedback adaptive controller.

1 Introduction

Although the position of a robot link can be measured accurately, the measurement of velocity and acceleration tends to result in noisy signals. In extreme cases, these signals could be so noisy that their use in the controller would no longer be feasible [1].

In order to overcome the problem of noisy velocity measurements and to guarantee that the error between the time-varying desired position and the actual position of the robot system goes asymptotically to zero for a set of initial conditions, a controller/observer scheme based on only position measurements can be used. In this sort of schemes, the incorporated observer is used to estimate the velocity signal and sometimes the acceleration signal.

Another approach consists in using Lyapunov's theory to design a controller/filter to guarantee the tracking of the desired trajectory, no matter if an estimate of the velocity and acceleration can be possible with the obtained design.

From the perspective of control engineering, the approach of using only joint position measurements either in a controller/observer or controller/filter to achieve tracking of a desired joint trajectory is denominated output feedback tracking control of robot manipulators. See textbooks [2, 3], which address that problem from an academic point of view.

Adaptive control of robot manipulators has been an active research topic in the last 15 years. The main motivation has been the interest in adding a reliable degree of robustness to the closed-loop system, which is specially important in the manufacturing processes, where the manipulator frequently achieves pick and place tasks of materials and parts, whereby adaptation to the payload changes helps to guarantee the motion control. See, for example, [4] for a reference on globally asymptotically stable adaptive algorithms, which guarantee the asymptotic tracking of the joint desired trajectory. However, in most of the adaptive controllers, measure of the joint velocity is assumed for feedback.

The problem of adaptive output feedback tracking control of manipulators consists in designing a control algorithm together with a parameter estimation update law by using only joint position measurements, so that the error between the time-varying desired position and the position of the system goes asymptotically to zero for a set of initial conditions. In this paper, such a control problem is addressed.

Much effort has been done in the design of full-state feedback adaptive controllers. However, the problem of design and analysis of output feedback adaptive control becomes more complicated, because of the absence of a damping factor introduced by the controller. That is why there are relatively few algorithms that combine both adaptive schemes and velocity reconstruction.

In relation to the literature review on output feedback adaptive control, we only cite papers published later than 1997. For schemes proposed before 1997, see the references in [5]. In the work by Zhang *et al.* [5, 6], an adaptive output feedback tracking controller depending on the initial condition of a dynamic extension was introduced. A redesign of that approach was proposed in the work of Zergeroglu *et al.* [7], but presenting the global convergence of the position and tracking errors. These approaches were extended later by Dixon *et al.* [8] to the problem of adaptive trajectory tracking control of manipulators with flexible joints by using only position measurements of the robot actuators and links. In a similar way, in that work the global convergence of the link position and velocity errors is shown. Recently, Artega [9] proposed an adaptive scheme with boundedness of the estimated parameters and uniform ultimate boundedness for tracking and observation errors. The work by Daly and Schwartz [1] reported the experimental results concerning three output feedback tracking controllers. They showed the advantages and disadvantages of each control scheme that was tested. Alonge *et al.* [10] proposed an adaptive controller based on a filtered signal to generate both the PD action and velocity estimates of the joints, which was experimentally tested.

The main aim of this paper is to introduce a new adaptive output feedback tracking controller for manipulators. The proposed controller presents the following features:

- If large enough viscous friction damping is present at the robot joints, the new controller guarantees the result of global convergence of the position and velocity tracking errors.
- Without relating the natural viscous friction damping, the controller is able to guarantee the local exponential convergence of the closed-loop solutions, which includes the robot parameter estimation error.
- Motivated by practical implications, the controller is designed considering that the applied torque is provided by

direct current (DC) motor actuators whose characteristics are unknown.

The theoretical contributions are described in the main propositions. Their proof is presented in a constructive and rigorous way, invoking Lyapunov analysis and the theory of singularly systems. In addition to the theoretical contributions, experimental tests in a DC motor-actuated horizontal two degrees-of-freedom direct-drive robot are presented. To compare the performance of the new controller, the experimental work includes the real-time implementation of the adaptive output feedback controller introduced in [7].

This paper is organised as follows. Section 2 deals with robot dynamics and the control problem formulation. In Section 3, the new output feedback adaptive control law and its analysis are introduced. The experimental results are described in Section 4. Finally, some concluding remarks are drawn in Section 5.

Notation: Throughout this paper, the following notation will be adopted. $\|x\| = \sqrt{x^T x}$ stands for the norm of vector $x \in \mathbb{R}^n$. $\lambda_{\min}\{A(x)\}$ and $\lambda_{\max}\{A(x)\}$ denote the minimum and maximum eigenvalues of a symmetric positive-definite matrix $A(x) \in \mathbb{R}^{n \times n}$ for all $x \in \mathbb{R}^n$, respectively.

$\|B(x)\| = \sqrt{\lambda_{\max}\{B(x)^T B(x)\}}$ stands for the induced norm of a matrix $B(x) \in \mathbb{R}^{m \times n}$ for all $x \in \mathbb{R}^n$. In this paper, the notation $\text{hypfunc}(x)$ denotes a hyperbolic function of $x \in \mathbb{R}$, for example, $\tanh(x)$ and $\ln(\cosh(x))$, while the notation $\text{Hypfunc}(z) = \text{diag}\{\text{hypfunc}(z_1), \dots, \text{hypfunc}(z_n)\}$, $z = [z_1, \dots, z_n]^T \in \mathbb{R}^n$, denotes a diagonal matrix containing as elements the hyperbolic function of each element of the vector z . As example, $\text{Sech}^2(z) = \text{diag}\{\text{sech}^2(z_1), \dots, \text{sech}^2(z_n)\}$. See Appendix 1 for the hyperbolic function properties used in this paper.

2 Robot dynamics, control goal and model properties

2.1 Robot dynamics

The dynamics in joint space of a serial-chain n -link robot manipulator considering the presence of friction at the robot joints can be written as [11, 12]

$$M(q)\ddot{q} + C(q, \dot{q})\dot{q} + g(q) + F_v \dot{q} = \tau \quad (1)$$

where $M(q) \in \mathbb{R}^{n \times n}$ is the symmetric positive-definite inertia matrix, $C(q, \dot{q}) \in \mathbb{R}^n$ is the vector of centripetal and Coriolis torques, $F_v \in \mathbb{R}^{n \times n}$ is a constant positive-definite diagonal matrix, which contains the viscous friction coefficients, $g(q) \in \mathbb{R}^n$ is the vector of gravitational torques and $\tau \in \mathbb{R}^n$ is the vector of applied torque inputs.

Without loss of generality, let us assume that the robot is actuated by permanent-magnet DC motors. In addition, for

a n degrees-of-freedom robot there are n DC motors that deliver torque at each robot joint. Usually, DC motors are operated by a servo amplifier in current mode, which makes the motor input current tend to the desired current in very short time. In other words, the current loop of the servo amplifier is tuned so that the electrical dynamics becomes much less dominant than the mechanical one.

The applied joint torques are directly related to the joint motor currents as

$$\tau(t) = K_m i_m(t)$$

where $i_m \in \mathbb{R}^n$ is the vector of the joint motor currents and $K_m \in \mathbb{R}^{n \times n}$ is a diagonal matrix containing the motor torque constants, which are usually difficult to estimate. By using servo amplifiers working in current mode, we can consider that the actual current is equal to the desired one, that is

$$i_m(t) = i_d(t) = K_{sa} u(t)$$

where $i_d(t) \in \mathbb{R}^n$ is the vector of the desired motor currents, $K_{sa} \in \mathbb{R}^{n \times n}$ is a diagonal matrix containing the servo amplifier gains, which are user defined and $u(t)$ the servo amplifier input voltage. Therefore the DC motor output torque is given as

$$\tau(t) = K_m K_{sa} u(t) = K u(t) \quad (2)$$

whereby the DC motor actuators can be modelled as ideal torque sources.

Finally, the robot model (1)–(2) can be written as

$$\overline{M}(q)\ddot{q} + \overline{C}(q, \dot{q})\dot{q} + \overline{g}(q) + \overline{F}_v\dot{q} = u \quad (3)$$

where the bar symbol denotes multiplication by K^{-1} . The results introduced in this paper consider that the positive-definite matrix $K \in \mathbb{R}^{n \times n}$ is unknown. To the best of the authors' knowledge, adaptive output feedback tracking control of the class of robots (3) has not been reported. In the robot model (3) the servo amplifier voltage vector $u \in \mathbb{R}^n$ is the control input.

2.2 Control goal

Assume that only robot joint displacements $q(t) \in \mathbb{R}^n$ are available for measurement and uncertainty on the robot parameters is present. Then, the adaptive output feedback tracking control problem consists in designing a control input $u \in \mathbb{R}^n$ together with a parameter estimation update law so that the limit

$$\lim_{t \rightarrow \infty} \tilde{q}(t) = 0 \quad (4)$$

is assured, where

$$\tilde{q}(t) = q_d(t) - q(t) \quad (5)$$

is the tracking error and $q_d(t) \in \mathbb{R}^n$ is the desired joint position trajectory.

Throughout this paper, we consider that the desired time-varying trajectory $q_d(t)$ is three times differentiable and is bounded for all time $t \geq 0$ in the sense

$$\|\dot{q}_d(t)\| \leq \mu_1 \quad (6)$$

$$\|\ddot{q}_d(t)\| \leq \mu_2 \quad (7)$$

where μ_1 and μ_2 denote known positive constants.

2.3 Properties on the robot model

Although the equation of motion (2) is complex, it is possible to show that it exhibits several fundamental properties that are exploited to facilitate control system design. In order to introduce such properties of the robot model (11), the following assumption will be important.

• *Assumption 1.* The product of the inverse of the motor and servo amplifier matrix K^{-1} and the inertia matrix $M(q)$ is a positive-definite matrix, that is

$$x^T \overline{M}(q)x = x^T K^{-1} M(q)x > 0, \quad \forall x \neq 0 \quad (8)$$

If the symmetric part of the matrix $\overline{M}(q)$ is used, the assumption (8) can be written as

$$x^T \overline{M}^*(q)x = x^T \overline{M}^*(q)x > 0, \quad \forall x \neq 0 \quad (9)$$

where

$$\overline{M}^*(q) = \frac{1}{2} [\overline{M}(q) + \overline{M}(q)^T] \quad (10)$$

The inertia matrix $M(q) \in \mathbb{R}^{n \times n}$ in model (1) is symmetric and positive definite. Assumption 1 states that if the DC motors and servo amplifiers have different characteristics, the matrix $\overline{M}(q) = K^{-1} M(q)$ will not be symmetric but positive definite. In many of the practical situations that we have found, this statement is true. From a practical point of view, Assumption 1 resembles a property more than an assumption.

Next, properties on the robot model (3) are given. The proof that the properties hold for the robot model (2) can be easily achieved by following the analysis in Section 4 and Appendix C of reference [12].

• *Property 1:* For all $q, \dot{q}, \ddot{q} \in \mathbb{R}^n$, we have that the robot model (2) can be parameterised as

$$\overline{M}(q)\ddot{q} + \overline{C}(q, \dot{q})\dot{q} + \overline{g}(q) + \overline{F}_v\dot{q} = Y(q, \dot{q}, \ddot{q})\theta = u \quad (11)$$

where $Y(q, \dot{q}, \ddot{q}) \in \mathbb{R}^{n \times r}$ is the regression matrix and the elements of the vector $\theta \in \mathbb{R}^r$ are the lumped equivalent parameters of the robot, which include the characteristics of the DC motor and the servo amplifier.

Let us notice that in [13] the regression form (11) of robot manipulators actuated by DC motors and current-mode servo amplifiers was used to implement identification methods to estimate the vector $\theta \in \mathbb{R}^r$.

• *Property 2:* For all $q, \dot{q}, x, y, z \in \mathbb{R}^n$, the inertia and Coriolis matrix (using Christoffel symbols) satisfy

$$\lambda_{\max}\{\overline{M}^*(q)\}\|x\|^2 \geq x^T \overline{M}^*(q) x \geq \lambda_{\min}\{\overline{M}^*(q)\}\|x\|^2 \quad (12)$$

with $\overline{M}^*(q)$ defined in (10),

$$\dot{\overline{M}}(q) = K^{-1}C(q, \dot{q}) + K^{-1}C(q, \dot{q})^T = \overline{C}(q, \dot{q}) + \overline{C}^*(q, \dot{q})^T \quad (13)$$

$$\overline{C}(x, y)z = \overline{C}(x, z)y \quad (14)$$

$$\overline{C}(x, y + z) = \overline{C}(x, y) + \overline{C}(x, z) \quad (15)$$

$$\|\overline{C}(q, \dot{q})\|, \|\overline{C}^*(q, \dot{q})\| \leq k_{C1}\|\dot{q}\| \quad (16)$$

$$x^T \left[\frac{1}{2} \dot{\overline{M}}(q) - \overline{C}(q, \dot{q}) \right] x = 0 \quad \text{only if } K = kI, \quad k > 0 \quad (17)$$

Note that an important property of the robot dynamics (1) is the well-known skew-symmetry property of the matrix $[(1/2)\dot{\overline{M}}(q) - \overline{C}(q, \dot{q})]$. However, in the class of robots actuated by DC motors in (3), such a property holds only under the assumption that matrix K has identical elements, (17).

• *Property 3:* The so-called residual dynamics [14, 15], is defined by

$$\begin{aligned} \overline{h}(\tilde{q}, \dot{\tilde{q}}) &= [\overline{M}(q_d) - \overline{M}(q)]\ddot{q}_d + [\overline{C}(q_d, \dot{q}_d) - \overline{C}(q, \dot{q})]\dot{q}_d \\ &\quad + [\overline{g}(q_d) - \overline{g}(q)] \end{aligned} \quad (18)$$

where $\tilde{q}(t)$ is defined in (5) and $q_d(t)$ is the desired joint position trajectory. The residual dynamics (18) satisfies the following inequality [12]

$$\|\overline{h}(\tilde{q}, \dot{\tilde{q}})\| \leq k_{C1}\mu_1\|\dot{\tilde{q}}\| + \frac{\delta\alpha}{\tanh(\alpha\sigma)}\|\tanh(\sigma\tilde{q})\| \quad (19)$$

where $\sigma > 0$, the constant μ_1 in (6) and

$$\delta = k_g + k_M\mu_2 + k_{C2}\mu_1^2 \quad (20)$$

$$\alpha = 2 \frac{k_1 + k_2\mu_2 + k_{C1}\mu_1^2}{\delta} \quad (21)$$

□

The constants involved in the robot model properties (12)–(19) can be computed as follows (Section 4 and Appendix C in [12] are referred again to see the steps for the derivation of the next inequalities)

$$k_M \geq n^2 \left[\max_{i,j,k,q} \left| \frac{\partial \overline{M}_{ij}(q)}{\partial q_k} \right| \right] \quad (22)$$

$$k_{C1} \geq n^2 \left[\max_{i,j,k,q} |\overline{c}_{ijk}(q)| \right] \quad (23)$$

$$k_{C2} \geq n^3 \left[\max_{i,j,k,l,q} \left| \frac{\partial \overline{c}_{ijk}(q)}{\partial q_l} \right| \right] \quad (24)$$

$$k_g \geq n \left[\max_{i,j,q} \left| \frac{\partial \overline{g}_i(q)}{\partial q_j} \right| \right] \quad (25)$$

$$k_1 \geq \sup_{\forall q \in \mathbb{R}^n} \|\overline{g}(q)\| \quad (26)$$

$$k_2 \geq \lambda_{\max}\{\overline{M}(q)\} \quad (27)$$

where $\overline{M}_{ij}(q)$ is the ij element of matrix $\overline{M}(q)$, $\overline{c}_{ijk}(q)$ is the ijk Christoffel symbol and $\overline{g}_i(q)$ is the i element of vector $\overline{g}(q)$.

3 Proposed controller and analysis

3.1 Adaptive output feedback tracking controller

Now, we are in a position to introduce the following adaptive output feedback tracking controller

$$u = Y(q_d, \dot{q}_d, \ddot{q}_d)\hat{\theta} + K_v \tanh(\tilde{\vartheta}) + K_p \tanh(\sigma\tilde{q}) \quad (28)$$

where \tilde{q} denotes the tracking error in (5), K_p and K_v are $n \times n$ positive-definite matrices, and constant $\sigma > 0$.

The signal $\tilde{\vartheta}(t)$ in the adaptive controller (28) is obtained from the following non-linear filter

$$\dot{x} = -A \tanh(\tilde{\vartheta}) \quad (29)$$

$$\tilde{\vartheta} = x + B\tilde{q} \quad (30)$$

where $x \in \mathbb{R}^n$, A and B are $n \times n$ positive-definite matrices.

The definition of the controller (28) is completed with the vector of estimated robot parameters $\hat{\theta}(t) \in \mathbb{R}^r$, which is

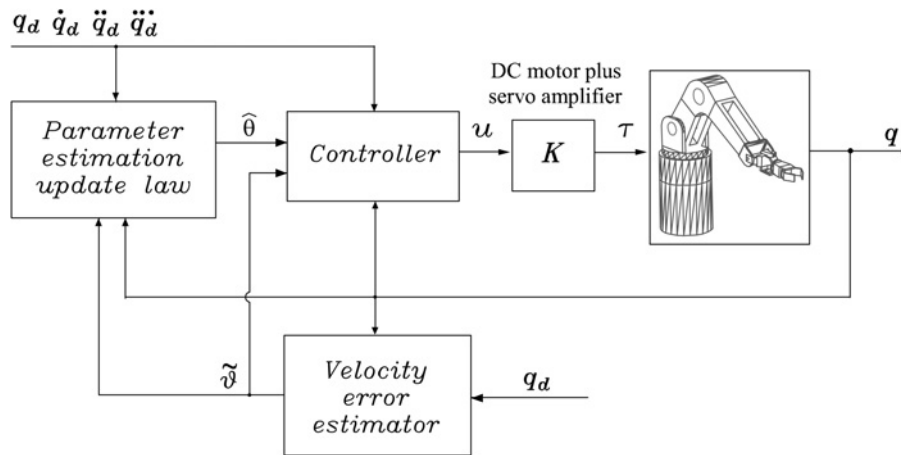


Figure 1 Block diagram of the adaptive output feedback tracking controller that uses only position measurements

obtained from the following update law

$$\hat{\theta} = \Gamma_a \left[Y^T(q_d, \dot{q}_d, \ddot{q}_d) \tilde{q} - \int_0^t [\dot{Y}^T(q_d, \dot{q}_d, \ddot{q}_d) \tilde{q} - \epsilon Y^T(q_d, \dot{q}_d, \ddot{q}_d) \tanh(\sigma \tilde{q})] dt \right] \quad (31)$$

with Γ_a a positive-definite matrix and the strictly positive constant $\epsilon \in (\epsilon_{\min}, \epsilon_{\max})$. The explicit values of ϵ_{\min} and ϵ_{\max} will be defined later. Fig. 1 shows a block diagram of the implementation of the controller (28)–(31).

Note that the adaptive controller (28) does not require measurement of the joint velocity $\dot{q} \in \mathbb{R}^n$. Instead, the non-linear filter (29)–(30) is implemented to obtain the joint velocity error-like signal $\tilde{v} \in \mathbb{R}^n$. As seen in the coming analysis, the proposed design in equations (28)–(31) is the result of using Lyapunov’s theory to guarantee the tracking of the desired trajectory, no matter if an estimate of the velocity and acceleration can be possible with the non-linear filter (29)–(30). In other words, the proposed controller, filter and parameter estimation update law are the results of a Lyapunov-function-based design.

3.2 Analysis

The closed-loop system can be obtained by substituting the controller equation (28) into the robots dynamics (2), using Property 1 of the robot model, differentiating (30) with respect to time, and using the definition

$$\tilde{\theta} = \theta - \hat{\theta} \in \mathbb{R}^r \quad (32)$$

whose time derivative is $\dot{\tilde{\theta}} = -\dot{\hat{\theta}}$. Then, we can write (see (33))

where $\bar{h}(\tilde{q}, \dot{\tilde{q}})$ is the residual dynamics in (18). The closed-loop system (33) is a non-linear and non-autonomous and the state-space origin $[\tilde{q}^T \dot{\tilde{q}}^T \tilde{v}^T \tilde{\theta}^T]^T = 0 \in \mathbb{R}^{3n+r}$ is an equilibrium point.

Let us define the constants

$$\gamma_1 = \frac{\delta \alpha}{\tanh(\alpha \sigma)} \quad (34)$$

$$\gamma_2 = 2k_{C1} \mu_1 + \lambda_{\max}\{\bar{F}_v\} \quad (35)$$

$$\gamma_3 = k_{C1} \sqrt{n} + \sigma \|\bar{M}(q)\| \quad (36)$$

where δ and α are defined in (20) and (21), respectively, and $\sigma > 0$ is the control parameter used in the controller (28).

The main results are stated in the remaining of this section. The first result is based under the assumptions of large enough viscous friction damping and on the servo amplifiers and DC motors that drive each degree-of-freedom are identical, that is, $K = kI$, $k > 0$. Thus, the global stability of the state-space origin of the system (33) is proven. In the second result, the assumptions on the robot model are relaxed, and then local exponential stability is guaranteed.

Proposition 1: Assume that the damping introduced by the viscous friction coefficients \bar{F}_v satisfies

$$\lambda_{\min}\{\bar{F}_v\} > k_{C1} \mu_1 \quad (37)$$

$$\frac{d}{dt} \begin{bmatrix} \tilde{q} \\ \dot{\tilde{q}} \\ \tilde{\theta} \\ \tilde{v} \end{bmatrix} = \begin{bmatrix} \dot{\tilde{q}} \\ \bar{M}(q)^{-1} \left[-\bar{C}(q, \dot{q}) \dot{\tilde{q}} - \bar{F}_v \dot{\tilde{q}} - K_v \tanh(\tilde{v}) - K_p \tanh(\sigma \tilde{q}) - \bar{h}(\tilde{q}, \dot{\tilde{q}}) + Y(q_d, \dot{q}_d, \ddot{q}_d) \tilde{\theta} \right] \\ -\Gamma_a Y(q_d, \dot{q}_d, \ddot{q}_d)^T [\dot{\tilde{q}} + \epsilon \tanh(\sigma \tilde{q})] \\ -A \tanh(\tilde{v}) + B \dot{\tilde{q}} \end{bmatrix} \quad (33)$$

where μ_1 is defined in (6) and k_{C1} is obtained as in (23), the gain K_p such that its smallest eigenvalue is large enough, and the gain $\epsilon \in (\epsilon_{\min}, \epsilon_{\max})$. In addition, assume that the voltage-to-torque conversion matrix K in (2) satisfies

$$K = kI \in \mathbb{R}^{n \times n}, \quad k > 0$$

Then, the closed-loop system (33) is globally uniformly stable. In addition, for any initial condition $[\tilde{q}(0)^T \dot{\tilde{q}}(0)^T \tilde{\vartheta}(0)^T \tilde{\theta}(0)^T]^T$, the limit

$$\lim_{t \rightarrow \infty} \begin{bmatrix} \tilde{q}(t) \\ \dot{\tilde{q}}(t) \\ \tilde{\vartheta}(t) \end{bmatrix} = 0$$

is assured, whereas $\tilde{\theta}(t)$ remains bounded for all time $t \geq 0$.

Proof: We propose the following Lyapunov function candidate

$$\begin{aligned} V(t, \tilde{q}, \dot{\tilde{q}}, \tilde{\vartheta}, \tilde{\theta}) &= \frac{1}{2} \dot{\tilde{q}}^T \overline{M}(q) \dot{\tilde{q}} + \sum_{i=1}^n k_{v_i} b_i^{-1} \ln(\cosh(\tilde{\vartheta}_i)) \\ &+ \sum_{i=1}^n k_{p_i} \sigma^{-1} \ln(\cosh(\sigma \tilde{q}_i)) \\ &+ \epsilon \tanh(\sigma \tilde{q})^T \overline{M}(q) \dot{\tilde{q}} + \frac{1}{2} \tilde{\theta}^T \Gamma_a^{-1} \tilde{\theta} \end{aligned} \quad (38)$$

where ϵ is the positive constant involved in the update law (31). Also notice that for all $x, q \in \mathbb{R}^n$, $x^T \overline{M}(q)x = x^T \overline{M}^*(q)x$, with $\overline{M}^*(q)$ the so-called symmetric part of $\overline{M}(q)$ given in (10). By using Assumption 1 in (8) and (9), Property 2 of the robot model and properties of hyperbolic functions (see Appendix 1), a lower bound on $V(t, \tilde{q}, \dot{\tilde{q}}, \tilde{\vartheta}, \tilde{\theta})$ is given by

$$V(t, \tilde{q}, \dot{\tilde{q}}, \tilde{\vartheta}, \tilde{\theta}) \geq \eta^T P \eta + \sum_{i=1}^n k_{v_i} b_i^{-1} \ln(\cosh(\tilde{\vartheta}_i)) + \frac{1}{2} \tilde{\theta}^T \Gamma_a^{-1} \tilde{\theta}$$

where

$$\eta = \begin{bmatrix} \sqrt{\sum_{i=1}^n \ln(\cosh(\sigma \tilde{q}_i))} \\ \|\dot{\tilde{q}}\| \end{bmatrix} \quad (39)$$

and

$$P = \begin{bmatrix} \sigma^{-1} \lambda_{\min}\{K_p\} & -\frac{\epsilon}{2} \sqrt{2} \lambda_{\max}\{\overline{M}^*(q)\} \\ -\frac{\epsilon}{2} \sqrt{2} \lambda_{\max}\{\overline{M}^*(q)\} & \frac{1}{2} \lambda_{\min}\{\overline{M}^*(q)\} \end{bmatrix}$$

with matrix $\overline{M}^*(q)$ defined in (9).

If P is positive definite, then the function $V(t, \tilde{q}, \dot{\tilde{q}}, \tilde{\vartheta}, \tilde{\theta})$ is globally positive definite and radially unbounded. By using

Sylvester's Theorem in [16, pp. 397–398], the sufficient and necessary condition for P to be positive definite is

$$0 < \epsilon < \frac{\sqrt{\sigma^{-1} \lambda_{\min}\{K_p\} \lambda_{\min}\{\overline{M}(q)\}}}{\lambda_{\max}\{\overline{M}^*(q)\}}$$

The time derivative of $V(t, \tilde{q}, \dot{\tilde{q}}, \tilde{\vartheta}, \tilde{\theta})$ along the closed-loop systems trajectories (33) is given by

$$\begin{aligned} \dot{V}(t, \tilde{q}, \dot{\tilde{q}}, \tilde{\vartheta}, \tilde{\theta}) &= \epsilon \tanh(\sigma \tilde{q})^T [-\overline{F}_v \dot{\tilde{q}} - K_v \tanh(\tilde{\vartheta}) \\ &- K_p \tanh(\sigma \tilde{q}) + \overline{C}^*(q, \dot{q})^T \dot{\tilde{q}} - \overline{b}(\tilde{q}, \dot{\tilde{q}})] \\ &+ \epsilon \sigma \dot{\tilde{q}}^T \text{Sech}^2(\sigma \tilde{q}) \overline{M}(q) \dot{\tilde{q}} - \dot{\tilde{q}}^T \overline{F}_v \dot{\tilde{q}} - \dot{\tilde{q}}^T \overline{b}(\tilde{q}, \dot{\tilde{q}}) \\ &- \tanh(\tilde{\vartheta})^T K_v B^{-1} A \tanh(\tilde{\vartheta}) \end{aligned}$$

where properties (13) and (17) were used. Note that the matrix $\overline{C}^*(q, \dot{q})^T$ that appears in $\dot{V}(t, \tilde{q}, \dot{\tilde{q}}, \tilde{\vartheta}, \tilde{\theta})$ was defined in (13).

To obtain further conclusions on the closed-loop stability, we compute an upper bound on each term of the Lyapunov function time derivative

$$\begin{aligned} -\dot{\tilde{q}}^T \overline{F}_v \dot{\tilde{q}} &\leq -\lambda_{\min}\{\overline{F}_v\} \|\dot{\tilde{q}}\|^2 \\ -\dot{\tilde{q}}^T \overline{b}(\tilde{q}, \dot{\tilde{q}}) &\leq k_{C1} \mu_1 \|\dot{\tilde{q}}\|^2 + \gamma_1 \\ &\quad \times \tanh(\sigma \tilde{q}) \|\dot{\tilde{q}}\| \\ -\tanh(\tilde{\vartheta})^T K_v B^{-1} A \tanh(\tilde{\vartheta}) &\leq -\lambda_{\min}\{K_v B^{-1} A\} \|\tanh(\tilde{\vartheta})\|^2 \\ \epsilon \tanh(\sigma \tilde{q})^T \overline{C}^*(q, \dot{q})^T \dot{\tilde{q}} &\leq \epsilon k_{C1} \|\dot{\tilde{q}}\| \|\tanh(\sigma \tilde{q})\| \|\dot{\tilde{q}}\| \\ &\leq \epsilon k_{C1} \sqrt{n} \|\dot{\tilde{q}}\|^2 \\ &\quad + \epsilon k_{C1} \mu_1 \|\tanh(\sigma \tilde{q})\| \|\dot{\tilde{q}}\| \\ \epsilon \sigma \dot{\tilde{q}}^T \text{Sech}^2(\sigma \tilde{q}) \overline{M}(q) \dot{\tilde{q}} &\leq \epsilon \sigma \|\overline{M}(q)\| \|\dot{\tilde{q}}\|^2 \\ -\epsilon \tanh(\sigma \tilde{q}) K_v \tanh(\tilde{\vartheta}) &\leq \epsilon \lambda_{\max}\{K_v\} \\ &\quad \times \|\tanh(\sigma \tilde{q})\| \|\tanh(\tilde{\vartheta})\| \\ -\epsilon \tanh(\sigma \tilde{q})^T K_p \tanh(\sigma \tilde{q}) &\leq -\epsilon \lambda_{\min}\{K_p\} \|\tanh(\sigma \tilde{q})\|^2 \\ -\epsilon \tanh(\sigma \tilde{q})^T \overline{F}_v \dot{\tilde{q}} &\leq \epsilon \lambda_{\max}\{\overline{F}_v\} \|\tanh(\sigma \tilde{q})\| \|\dot{\tilde{q}}\| \\ -\epsilon \tanh(\sigma \tilde{q})^T \overline{b}(\tilde{q}, \dot{\tilde{q}}) &\leq \epsilon k_{C1} \mu_1 \|\tanh(\sigma \tilde{q})\| \|\dot{\tilde{q}}\| \\ &\quad + \epsilon \gamma_1 \|\tanh(\sigma \tilde{q})\|^2 \end{aligned} \quad (40)$$

where γ_1 is defined in (34). The bounds in (40) were obtained by using the inequality (16), Property 3 of the residual dynamics $\overline{b}(\tilde{q}, \dot{\tilde{q}})$, the fact $\|\dot{\tilde{q}}\| \leq \mu_1 + \|\dot{\tilde{q}}\|$, and properties of the hyperbolic functions in Appendix 1.

By grouping the bounds in (40) in a proper way, an upper bound on $\dot{V}(t, \tilde{q}, \dot{\tilde{q}}, \tilde{\vartheta}, \dot{\tilde{\vartheta}})$ can be written as

$$\dot{V}(t, \tilde{q}, \dot{\tilde{q}}, \tilde{\vartheta}, \dot{\tilde{\vartheta}}) \leq - \begin{bmatrix} \|\tanh(\sigma\tilde{q})\| \\ \|\dot{\tilde{q}}\| \\ \|\tanh(\tilde{\vartheta})\| \end{bmatrix}^T Q \begin{bmatrix} \|\tanh(\sigma\tilde{q})\| \\ \|\dot{\tilde{q}}\| \\ \|\tanh(\tilde{\vartheta})\| \end{bmatrix}$$

where $Q \in \mathbb{R}^{3 \times 3}$ is a symmetric matrix explicitly given by (see equation at the bottom of the page)

where γ_1 , γ_1 and γ_3 are given in (34), (35) and (36), respectively.

However, to facilitate the obtention of conditions on the negative semidefiniteness of $\dot{V}(t, \tilde{q}, \dot{\tilde{q}}, \tilde{\vartheta}, \dot{\tilde{\vartheta}})$, we have decided to write (see (41))

Sylvester's Theorem in [16, pp. 397–398], is used to obtain conditions in ϵ are that Q_1 and Q_2 are positive-definite matrices. To avoid a square condition in ϵ , the matrix Q_1 is written as (see (41))

$$Q_1 = \begin{bmatrix} \frac{\epsilon}{4}[\lambda_{\min}\{K_p\} - \gamma_1] & -\frac{1}{2}\gamma_1 \\ -\frac{1}{2}\gamma_1 & [1 - \beta]\lambda_{\min}\{\bar{F}_v\} \end{bmatrix} + \begin{bmatrix} \frac{\epsilon}{4}[\lambda_{\min}\{K_p\} - \gamma_1] & -\frac{1}{2}\epsilon\gamma_2 \\ -\frac{1}{2}\epsilon\gamma_2 & \beta\lambda_{\min}\{\bar{F}_v\} - k_{C1}\mu_1 - \epsilon\gamma_3 \end{bmatrix}$$

where $\beta \in (0,1)$. Then, the sufficient condition for Q_1 to be positive definite are

$$\epsilon > \frac{\gamma_1^2}{[1 - \beta][\lambda_{\min}\{K_p\} - \gamma_1]\lambda_{\min}\{\bar{F}_v\}}$$

$$\epsilon < \frac{[\lambda_{\min}\{K_p\} - \gamma_1][\beta\lambda_{\min}\{\bar{F}_v\} - k_{C1}\mu_1]}{[\lambda_{\min}\{K_p\} - \gamma_1]\gamma_3 + \gamma_2^2}$$

Finally, the sufficient and necessary condition for Q_2 to be positive definite is

$$\epsilon < \frac{2[\lambda_{\min}\{K_p\} - \gamma_1]\lambda_{\min}\{K_v B^{-1}A\}}{\lambda_{\max}\{K_v\}^2}$$

Then, for all (see (42))

the matrices P , Q_1 and Q_2 are positive definite, which implies that the $V(t, \tilde{q}, \dot{\tilde{q}}, \tilde{\vartheta}, \dot{\tilde{\vartheta}})$ is globally positive definite and radially unbounded function, and that its time derivative $\dot{V}(t, \tilde{q}, \dot{\tilde{q}}, \tilde{\vartheta}, \dot{\tilde{\vartheta}})$ is globally negative semidefinite. Therefore the state-space origin of the closed-loop system (33) is globally uniformly stable; see Theorem A.5 in [17, pp. 490].

Besides, we have that

$$[\tilde{q}(t)^T \dot{\tilde{q}}(t)^T \tilde{\vartheta}(t)^T \dot{\tilde{\vartheta}}(t)^T]^T, [\dot{\tilde{q}}(t)^T \ddot{\tilde{q}}(t)^T \ddot{\tilde{\vartheta}}(t)^T \dot{\tilde{\vartheta}}(t)^T]^T \in L_\infty^{3n+r}$$

that is, the solution of the closed-loop system and its time

$$Q = \begin{bmatrix} \epsilon[\lambda_{\min}\{K_p\} - \gamma_1] & -\frac{1}{2}\gamma_1 - \frac{1}{2}\epsilon\gamma_2 & -\frac{\epsilon}{2}\lambda_{\max}\{K_v\} \\ -\frac{1}{2}\gamma_1 - \frac{1}{2}\epsilon\gamma_2 & \lambda_{\min}\{\bar{F}_v\} - k_{C1}\mu_1 - \epsilon\gamma_3 & 0 \\ -\frac{\epsilon}{2}\lambda_{\max}\{K_v\} & 0 & \lambda_{\min}\{K_v B^{-1}A\} \end{bmatrix}$$

$$\dot{V}(t, \tilde{q}, \dot{\tilde{q}}, \tilde{\vartheta}, \dot{\tilde{\vartheta}}) \leq - \begin{bmatrix} \|\tanh(\sigma\tilde{q})\| \\ \|\dot{\tilde{q}}\| \end{bmatrix}^T \underbrace{\begin{bmatrix} \frac{\epsilon}{2}[\lambda_{\min}\{K_p\} - \gamma_1] & -\frac{1}{2}\gamma_1 - \frac{1}{2}\epsilon\gamma_2 \\ -\frac{1}{2}\gamma_1 - \frac{1}{2}\epsilon\gamma_2 & \lambda_{\min}\{\bar{F}_v\} - k_{C1}\mu_1 - \epsilon\gamma_3 \end{bmatrix}}_{Q_1} \begin{bmatrix} \|\tanh(\sigma\tilde{q})\| \\ \|\dot{\tilde{q}}\| \end{bmatrix} - \begin{bmatrix} \|\tanh(\sigma\tilde{q})\| \\ \|\tanh(\tilde{\vartheta})\| \end{bmatrix}^T \underbrace{\begin{bmatrix} \frac{\epsilon}{2}[\lambda_{\min}\{K_p\} - \gamma_1] & -\frac{\epsilon}{2}\lambda_{\max}\{K_v\} \\ -\frac{\epsilon}{2}\lambda_{\max}\{K_v\} & \lambda_{\min}\{K_v B^{-1}A\} \end{bmatrix}}_{Q_2} \begin{bmatrix} \|\tanh(\sigma\tilde{q})\| \\ \|\tanh(\tilde{\vartheta})\| \end{bmatrix} \tag{41}$$

$$\frac{\gamma_1^2}{[1 - \beta][\lambda_{\min}\{K_p\} - \gamma_1]\lambda_{\min}\{\bar{F}_v\}} < \epsilon < \min \left\{ \frac{[\lambda_{\min}\{K_p\} - \gamma_1][\beta\lambda_{\min}\{\bar{F}_v\} - k_{C1}\mu_1]}{[\lambda_{\min}\{K_p\} - \gamma_1]\gamma_3 + \gamma_2^2}, \frac{2[\lambda_{\min}\{K_p\} - \gamma_1]\lambda_{\min}\{K_v B^{-1}A\}}{\lambda_{\max}\{K_v\}^2}, \frac{\sqrt{\sigma^{-1}\lambda_{\min}\{K_p\}\lambda_{\min}\{M(\tilde{q})\}}}{\lambda_{\max}\{M(\tilde{q})\}} \right\} \tag{42}$$

derivative are bounded functions. Therefore the solution of the closed-loop system is a uniformly bounded function. Integrating both sides of inequality (41), it can be shown that

$$\frac{V(t_0)}{\min\{\lambda_{\min}\{Q_1\}, \lambda_{\min}\{Q_2\}\}} \geq \int_{t_0}^t \left\| \left[\|\tanh(\sigma\tilde{q}(t))\| \|\dot{\tilde{q}}(t)\| \|\tilde{\vartheta}(t)\| \right]^T \right\|^2 dt$$

which means $[\tilde{q}(t)^T \dot{\tilde{q}}(t)^T \tilde{\vartheta}(t)^T]^T \in L_2^{3n}$ and the limit

$$\lim_{t \rightarrow \infty} \int_0^\infty [\tilde{q}(\sigma)^T \dot{\tilde{q}}(\sigma)^T \tilde{\vartheta}(\sigma)^T]^T d\sigma$$

exists. Hence, by invoking Barbalat's lemma [18], we conclude

$$\lim_{t \rightarrow \infty} \begin{bmatrix} \tilde{q}(t) \\ \dot{\tilde{q}}(t) \\ \tilde{\vartheta}(t) \end{bmatrix} = 0$$

which completes the proof of Proposition 1. □

It is noteworthy that some global stability results based on a condition relating the viscous friction damping \bar{F}_v and the bound of the desired joint velocity $\|\dot{q}_d(t)\| < \mu_1$ have been reported. In [19] a 'non-adaptive' output feedback controller was introduced. Recently, in [20] the proof that PD controller plus feedforward solves the global output feedback tracking control problem was provided, and in [21] a class of global full-state feedback saturated controllers was proposed. However, these works did not address the extension to global adaptive output feedback tracking control, as is done in the present paper.

If condition (37) is not satisfied, that is, if the viscous friction damping \bar{F}_v is low and the requested task has high speed $\|\dot{q}_d(t)\|$ such that μ_1 in (6) is large, the global convergence result cannot be guaranteed by Proposition 1. Also, a situation that can arise in practice is the use of DC motors and servo amplifiers with different features to drive the robot joints. This means that the voltage to torque matrix $K \in \mathbb{R}^{n \times n}$ has different elements and the property of skew-symmetry of the matrix $[\frac{1}{2}\bar{M}(q) - \bar{C}(q, \dot{q})]$ written in (17) is no longer valid. However, although condition (37) is not satisfied and DC motors and servo amplifiers with different characteristics are used, the new controller (28)–(31) posses the important property of assuring exponential convergence of the error signals

$[\tilde{q}(t)^T \dot{\tilde{q}}(t)^T \tilde{\vartheta}(t)^T \tilde{\vartheta}(t)^T]^T$ for a local set of initial conditions. As shown later, this statement can be derived by using the theory of singularly perturbed systems [18].

In order to introduce the second main result, note that by the selection of gain

$$\epsilon = \epsilon_1 + \epsilon_2 \tag{43}$$

which is related to the parameter estimation update law (31), and the filter gains

$$A = B = \frac{1}{\epsilon_1} \tag{44}$$

the closed-loop system (33) can be rewritten as (see (45))

$$\epsilon_1 \frac{d}{dt} \tilde{\vartheta} = -\tanh(\tilde{\vartheta}) + \dot{\tilde{q}} \tag{46}$$

which has the standard form of a singularly perturbed system [18], where the gain ϵ_1 is the perturbing parameter. In general, a singularly perturbed system can be interpreted as a system composed by a slow dynamics subsystem and a fast dynamics subsystem. Now, we are in a position to establish the following result.

Proposition 2: Assume a selection of the gain matrices K_p and K_v such that their smallest eigenvalues are large enough. In addition, assume that the matrix $K \in \mathbb{R}^{n \times n}$ has different elements and that $Y(q_d, \dot{q}_d, \ddot{q}_d)$ is persistently exciting (PE), that is, there exist $a > 0$ and $T > 0$ such that [22]

$$\int_t^{t+T} Y_d(\rho)^T Y_d(\rho) d\rho \geq aI, \quad \forall t \in \mathbb{R}^+$$

$Y_d(t) = Y(q_d(t), \dot{q}_d(t), \ddot{q}_d(t))$. Then, there always exists $\epsilon_1^* > 0$ such that, for small enough $\epsilon_1^* > \epsilon_1 > 0$, the state-space origin of the closed-loop system (45)–(46) is locally exponentially stable.

Proof: Theorem 9.3 of [18], which is related to the stability of singularly perturbed systems, will be invoked. The conditions required to apply such theorem are presented in an itemised form:

1. Similar to the analysis of the closed-loop system (33), the state-space origin is an equilibrium point of the system (45)–(46).

$$\frac{d}{dt} \begin{bmatrix} \tilde{q} \\ \dot{\tilde{q}} \\ \tilde{\vartheta} \end{bmatrix} = \begin{bmatrix} \dot{\tilde{q}} \\ \bar{M}(q)^{-1} [-\bar{C}(q, \dot{q})\dot{\tilde{q}} - \bar{F}_v \dot{\tilde{q}} - K_v \tanh(\tilde{\vartheta}) - K_p \tanh(\sigma\tilde{q}) - \bar{h}(\tilde{q}, \dot{\tilde{q}}) + Y(q_d, \dot{q}_d, \ddot{q}_d)\tilde{\vartheta}] \\ -\Gamma_a Y(q_d, \dot{q}_d, \ddot{q}_d)^T [\dot{\tilde{q}} + [\epsilon_1 + \epsilon_2] \tanh(\sigma\tilde{q})] \end{bmatrix} \tag{45}$$

2. When $\epsilon_1 = 0$, we obtain the quasi-steady-state equation

$$0 = \tanh(\tilde{\vartheta}) + \dot{\tilde{q}} \tag{47}$$

which is an isolated root.

3. The right-hand side of (45)–(46) has bounded partial derivatives on compact sets.

4. With equations (45) and (47), the slow dynamics becomes (see (48))

For the sake of compactness of the paper, the proof that the state-space origin of (48) is locally exponentially stable will be outlined. The proof is done along the lines of Theorem 1 and Proposition 3 in [22], where a class of full-state feedback adaptive controllers for manipulators that leads to the closed-loop system with structure

$$\frac{d}{dt} \begin{bmatrix} x_1 \\ x_2 \end{bmatrix} = \begin{bmatrix} A(t, x_1) + B(t, x_1, x_2) \\ H(t, x_1, x_2) \end{bmatrix} \tag{49}$$

is studied. The slow dynamics (48) has the same structure of the system (49). Consider the Lyapunov function candidate

$$V(t, \tilde{q}, \dot{\tilde{q}}, \tilde{\theta}) = \frac{1}{2} \tilde{q}^T \overline{M}(q) \tilde{q} + \sum_{i=1}^n k_{p_i} \sigma^{-1} \ln(\cosh(\sigma \tilde{q}_i)) + \epsilon_2 \tanh(\sigma \tilde{q})^T \overline{M}(q) \dot{\tilde{q}} + \frac{1}{2} \tilde{\theta}^T \Gamma_a^{-1} \tilde{\theta} \tag{50}$$

which, assuming large enough $\lambda_{\min}\{K_p\}$, is a positive-definite, radially unbounded and decrescent function. It is possible to show that with large enough $\lambda_{\min}\{K_p\}$ and $\lambda_{\min}\{K_v\}$, properties of the robot model and properties of the hyperbolic functions, the time derivative of $V(t, \tilde{q}, \dot{\tilde{q}}, \tilde{\theta})$ achieves the upper bound

$$\dot{V}(t, \tilde{q}, \dot{\tilde{q}}, \tilde{\theta}) \leq -U(\tilde{q}, \dot{\tilde{q}}) \tag{51}$$

with $U(\tilde{q}, \dot{\tilde{q}})$ being a locally positive-definite function in its argument. For self contents of the paper, in Appendix 2 the proof of the inequality (51) is found. The local nature of the stability proof relays in observing that the skew-symmetry property of the bracketed matrix in (17) does not hold if the matrix $K \in \mathbb{R}^{n \times n}$ has different elements. In this way, a cubic term in the velocity error $\dot{\tilde{q}}(t) \in \mathbb{R}^n$, appears in the time-derivative of (50). Such a term can only be dominated locally by the term $K_v \tilde{q}(t) \in \mathbb{R}^n$, which comes from the second equation in (48). As pointed out, Appendix 2 is referred for the derivation of (51).

Inequality (51) shows that the state-space origin of the reduced system (48) is locally uniformly stable. Besides, it is possible to show that $\overline{M}(q_d) Y_d \tilde{\theta}$ is continuously differentiable and uniformly bounded in t on each compact set of the state. Then, by Theorem 1 in [22], the reduced system (48) is locally uniformly asymptotically stable if and only if the vector $\overline{M}(q_d) Y_d \tilde{\theta}$ is uniformly δ -persistently exciting (U δ -PE). However, as pointed in [22], $\overline{M}(q_d) Y_d \tilde{\theta}$ is U δ -PE if and only if $Y_d(t)$ is PE. Finally, by Proposition 3 (and its proof) in [22], the uniform local asymptotic stability of the state-space origin of (48), the assumption that $Y_d(t)$ is PE and the fact that the closed-loop system (48) is linearly uniformly bounded in t on each compact set of the state, the state-space origin of (48) is locally exponentially stable.

5. On the other hand, the boundary layer model is

$$\frac{d}{d\varsigma} \tilde{\vartheta} = -\tanh(\tilde{\vartheta}) + \dot{\tilde{q}} \tag{52}$$

where $\varsigma = t/\epsilon_1$ and $\dot{\tilde{q}}$ is interpreted as a constant. Let us define the function $W(\tilde{\vartheta}_i) = \frac{1}{2} [\tanh(\tilde{\vartheta}_i) - \dot{\tilde{q}}_i]^2$, whose derivative with respect to the scaled time $\varsigma = t/\epsilon_1$ satisfies the upper bound $(d/d\varsigma)W(\tilde{\vartheta}_i) \leq -\bar{k}W(\tilde{\vartheta}_i)$, which by the comparison lemma [18] implies that $[\tanh(\tilde{\vartheta}(\varsigma)) - \dot{\tilde{q}}] \rightarrow 0$ with exponential convergence rate as the scaled time $\varsigma = t/\epsilon_1$ increases.

By Theorem 9.3 in [18], there are sufficient conditions to claim the existence of ϵ_1^* such that $\epsilon_1^* > \epsilon_1 > 0$ guarantees the local exponential stability of the state-space origin of the system (45)–(46). \square

It is worthwhile to note that the result stated in Proposition 2 is valid for either equal or different characteristics of the actuators used. Thus, whether the skew-symmetry property of the matrix $[\frac{1}{2}\overline{M}(q) - \overline{C}(q, \dot{q})]$ is satisfied or not, the state-space origin of the closed-loop system (45)–(46) is locally exponentially stable.

3.3 Tuning guidelines

Procedure 1: Inspired from the results in Proposition 1, and assuming that condition (37) is satisfied and the voltage-to-torque matrix $K = kI \in \mathbb{R}^{n \times n}$, $k > 0$, the following practical tuning procedure is proposed:

1. Select the desired joint trajectory $q_d(t)$.
2. Select K_p large enough in order to obtain the set of value of ϵ in (42).

$$\frac{d}{dt} \begin{bmatrix} \tilde{q} \\ \dot{\tilde{q}} \\ \tilde{\theta} \end{bmatrix} = \begin{bmatrix} \dot{\tilde{q}} \\ \overline{M}(q)^{-1} \left[-\overline{C}(q, \dot{q}) \dot{\tilde{q}} - \overline{F}_v \dot{\tilde{q}} - K_v \dot{\tilde{q}} - K_p \tanh(\sigma \tilde{q}) - \overline{b}(\tilde{q}, \dot{\tilde{q}}) + Y(q_d, \dot{q}_d, \ddot{q}_d) \tilde{\theta} \right] \\ -\Gamma_a Y(q_d, \dot{q}_d, \ddot{q}_d)^T [\dot{\tilde{q}} + \epsilon_2 \tanh(\sigma \tilde{q})] \end{bmatrix} \tag{48}$$

3. Select ϵ .
4. Select σ , K_v and Γ_a .
5. Go to steps 2, 3 or 4 if the performance has to be improved.

Procedure 2: If condition (37) is not satisfied and either similar or different DC motors and servo amplifier gains are used as robot actuators, the result established in Proposition 2 is useful to tune the gains of controller (28)–(31):

1. Select the desired joint trajectory $q_d(t)$ so that $Y(q_d, \dot{q}_d, \ddot{q}_d)$ is persistently exciting.
2. Select small enough ϵ_1 , which at the same time sets the values for A and B as seen in (44).
3. Select a small enough ϵ_2 .
4. Compute ϵ from (43).
5. Select a large enough K_p and K_v .
6. Select σ and Γ_a .
7. Go to steps 2, 3, 4, 5 or 6 if the performance has to be improved.

4 Experimental results

A planar two degrees-of-freedom direct-drive arm has been built at the CITEDIPN Research Center. See Fig. 2 for a CAD drawing and picture. The system is composed of two DC *Pittman* motors operated in current mode with two Advanced Motion Controls servo amplifiers. A Sensoray 626 I/O card is used to read encoder signals with quadrature included and to transfer control commands through the D/A channels. A PC running Windows XP, Matlab, Simulink and Real-Time Windows Target is used to execute controllers in real-time with a 1 kHz sampling rate.

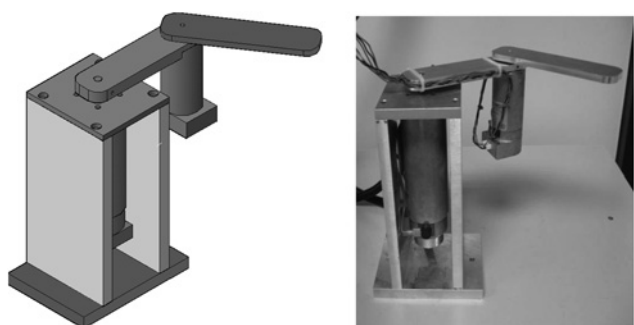


Figure 2 Experimental robot manipulator actuated by DC motors

Specifically, the robot model entries are given by

$$\overline{M}(q) = \begin{bmatrix} \theta_1 + 2\theta_2 \cos(q_2) & \theta_3 + \theta_2 \cos(q_2) \\ \theta_4 + \theta_5 \cos(q_2) & \theta_6 \end{bmatrix} \quad (53)$$

$$\overline{C}(q, \dot{q}) = \begin{bmatrix} -\theta_2 \sin(q_2) \dot{q}_2 & -\theta_2 \sin(q_2) [\dot{q}_1 + \dot{q}_2] \\ \theta_5 \sin(q_2) \dot{q}_1 & 0 \end{bmatrix} \quad (54)$$

$$\overline{F}_v = \text{diag}\{\theta_7, \theta_8\} \quad (55)$$

It is easy to show that the experimental robot arm with elements (53)–(55) achieves Property 1 in (11).

The elements of the regression matrix $Y(q, \dot{q}, \ddot{q})$ are

$$\begin{aligned} Y_{11} &= \ddot{q}_1, & Y_{21} &= 0 \\ Y_{12} &= \cos(q_2)[2\ddot{q}_1 + \ddot{q}_2] \\ &\quad - \sin(q_2)\dot{q}_2[2\dot{q}_1 + \dot{q}_2], & Y_{22} &= 0 \\ Y_{13} &= \ddot{q}_2, & Y_{23} &= 0 \\ Y_{14} &= 0, & Y_{24} &= \ddot{q}_1 \\ Y_{15} &= 0, & Y_{25} &= \cos(q_2)\ddot{q}_1 + \sin(q_2)\dot{q}_1^2 \\ Y_{16} &= 0, & Y_{26} &= \ddot{q}_2 \\ Y_{17} &= \dot{q}_1, & Y_{27} &= 0 \\ Y_{18} &= 0, & Y_{28} &= \dot{q}_2 \end{aligned} \quad (56)$$

By using the least-squares identification method [23], we have estimated the coefficients involved in the robot model (53)–(55), whose numerical value is shown in Table 1. This information was useful to select the gains and to carry out numerical simulations of the controllers to be tested.

The desired position trajectories for links 1 and 2 in the experiments were selected as follows [7]

$$q_d(t) = \begin{bmatrix} 1.0 \sin(3.5t)[1 - e^{-0.05t^3}] \\ 1.0 \sin(3.5t)[1 - e^{-0.05t^3}] \end{bmatrix} (\text{rad}) \quad (57)$$

Table 1 Estimated parameters of the experimental robot arm; see (53)–(55) for reference

Parameter	Value	Unit
θ_1	0.0480	$\text{s}^2 \text{ V/rad}$
θ_2	0.0038	$\text{s}^2 \text{ V/rad}$
θ_3	0.0033	$\text{s}^2 \text{ V/rad}$
θ_4	0.0157	$\text{s}^2 \text{ V/rad}$
θ_5	0.0227	$\text{s}^2 \text{ V/rad}$
θ_6	0.0166	$\text{s}^2 \text{ V/rad}$
θ_7	0.0141	V-s/rad
θ_8	0.0139	V-s/rad

which exhibits a motion profile without abrupt changes in position, velocity and acceleration.

In order to assess the performance of the proposed adaptive controller in (28), we have carried out experiments with an adaptive output feedback controller already proposed in the literature. Next, the details of the implementations are provided.

4.1 Experimental test of the controller proposed by Zergeroglu et al. [7]

Considering robot manipulators modelled as (2) and the fact of no repeated parameters θ_i in each joint equation of the experimental robot, the controller proposed in [7], Section 4, can be written in our notation as

$$u = Y(q_d, \dot{q}_d, \ddot{q}_d)\hat{\theta} - K_f \operatorname{col}\left\{\frac{y_i}{[1 - y_i^2]^2}\right\} + K_{\alpha 4} \tanh(\tilde{q}), \tag{58}$$

with matrix $K_f = \operatorname{diag}\{k_{f1}, \dots, k_{fn}\} > 0$, $\operatorname{col}\{x_i\} = [x_1 \dots x_n]^T$, scalar constants $\alpha_1, \alpha_2, \alpha_3 > 0$, matrix $K_{\alpha 4} = \operatorname{diag}\{\alpha_{41}, \dots, \alpha_{4n}\} > 0$, and the signal y_i obtained from the filter

$$\begin{aligned} \dot{p}_i = & -[1 - [p_i - k_{fi}\tilde{q}_i]^2][\alpha_3[p_i - k_{fi}\tilde{q}_i] - \alpha_2\alpha_{4i} \tanh(\tilde{q}_i)] \\ & - k_{fi}[\alpha_1 \tanh(\tilde{q}_i) + \alpha_2[p_i - k_{fi}\tilde{q}_i]] \end{aligned} \tag{59}$$

$$y_i = p_i - k_{fi}\tilde{q}_i, \quad i = 1, \dots, n, \tag{60}$$

k_{fi} being the elements of the gain matrix K_f used in the controller (58), and the adaptation law to estimate the unknown parameters

$$\begin{aligned} \dot{\hat{\theta}} = & \Gamma_a \left[Y(q_d, \dot{q}_d, \ddot{q}_d)^T \tilde{q} + \int_0^t [Y(q_d, \dot{q}_d, \ddot{q}_d)^T [\alpha_1 \tanh(\tilde{q}) + \alpha_2 y] \right. \\ & \left. - \dot{Y}(q_d, \dot{q}_d, \ddot{q}_d)^T \tilde{q}] dt \right] \end{aligned} \tag{61}$$

with the matrix $\Gamma_a = \Gamma_a^T > 0$ and $p(0) = k\tilde{q}(0)$.

By using the numerical values of the parameters in Table 1, we achieved numerical simulations of the controller (58)–(61), hereafter referred to as ZDQK controller, to find a set of gains for which an acceptable performance of the tracking errors was obtained. Specifically, the ZDQK

controller was implemented with

$$K_f = \operatorname{diag}\{2.0, 2.0\} \tag{62}$$

$$\alpha_1 = 1.0 \tag{63}$$

$$\alpha_2 = 1.0 \tag{64}$$

$$\alpha_3 = 1.0 \tag{65}$$

$$K_{\alpha 4} = \operatorname{diag}\{7.0, 10.0\} \tag{66}$$

and

$$\Gamma_a = \operatorname{diag}\{0.1, 0.02, 0.025, 0.002, 0.03, 0.04, 0.01, 0.01\} \tag{67}$$

The results are shown in Fig. 3, which depicts the position errors $\tilde{q}_1(t)$ and $\tilde{q}_2(t)$, and Fig. 4, which shows the time

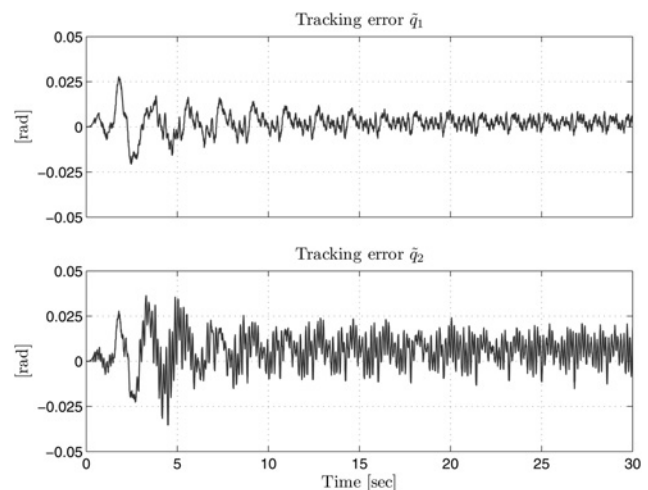


Figure 3 ZDQK controller: tracking errors $\tilde{q}_1(t)$ and $\tilde{q}_2(t)$

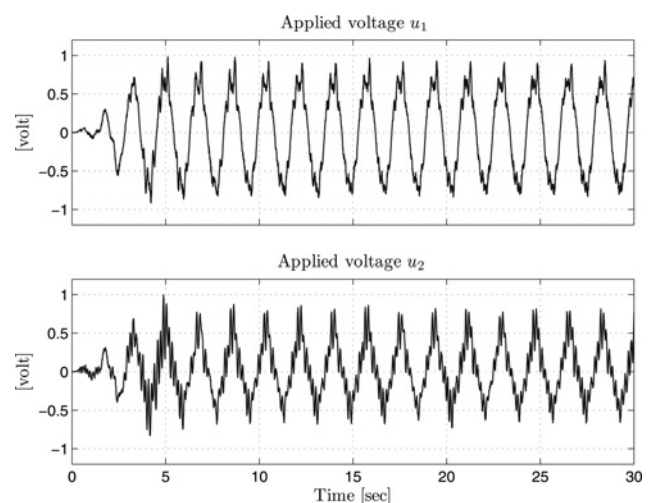


Figure 4 ZDQK controller: applied voltages $u_1(t)$ and $u_2(t)$

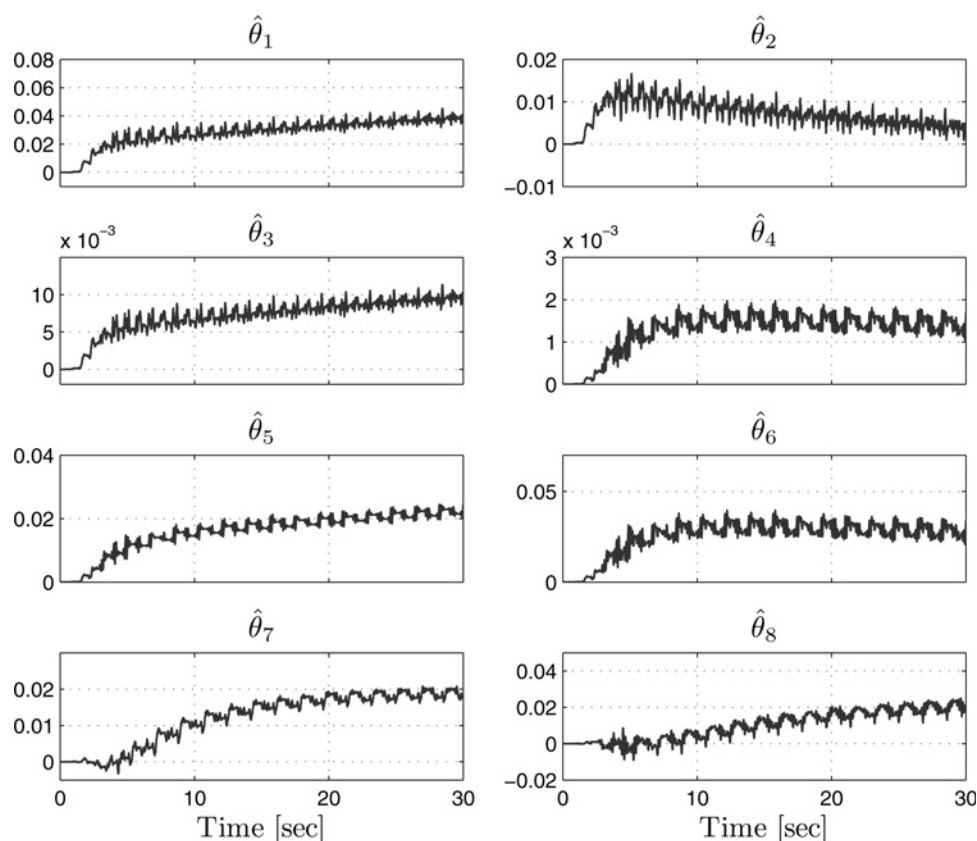


Figure 5 ZDQK controller: Estimated parameters $\hat{\theta}_i(t)$. See Table 1 for the units of each parameter

history of the applied control voltages $u_1(t)$ and $u_2(t)$. Besides, Fig. 5 illustrates the time evolution of the estimated parameters $\hat{\theta}_i(t)$, $i = 1, \dots, 8$.

4.2 Experimental test of the new controller

The experimental robot arm is equipped with DC motors and servo amplifiers with different characteristics. Thus, to select the gains of the new controller, we have resorted to the tuning Procedure 2 in Section 3.3, which was derived from Proposition 2.

The new controller was implemented with the desired trajectory $q_d(t)$ in (57). Since $q_d(t)$ is periodic, the matrix $Y_d(q_d, \dot{q}_d, \ddot{q}_d)$ is also periodic and in consequence is persistently exciting. We have selected $\epsilon_1 = 0.01$, which gives

$$A = B = \frac{1}{\epsilon_1} = 100.0$$

and $\epsilon_2 = 0.04$. These choices give $\epsilon = 0.5$ to be used in the update law (31). Although the structures of the ZDQK scheme and the new controller are different, we have tried to keep similar conditions in the

implementations. We used

$$K_p = K_{\alpha 4}$$

where $K_{\alpha 4}$ in (66) is the proportional gain in the ZDQK controller. In addition

$$K_v = \text{diag}\{0.4, 0.4\}$$

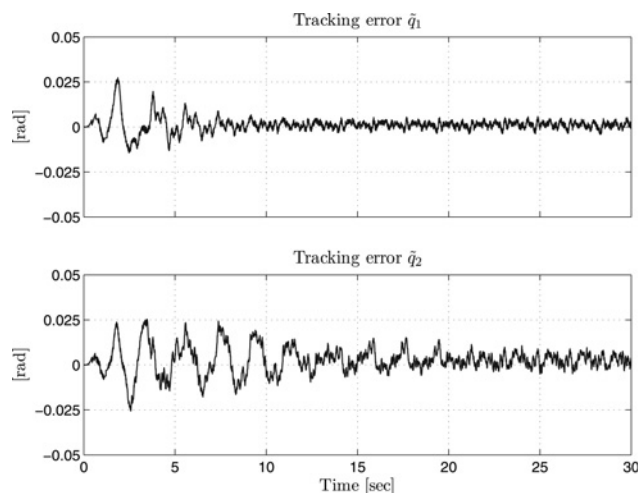


Figure 6 New controller: tracking errors $\tilde{q}_1(t)$ and $\tilde{q}_2(t)$

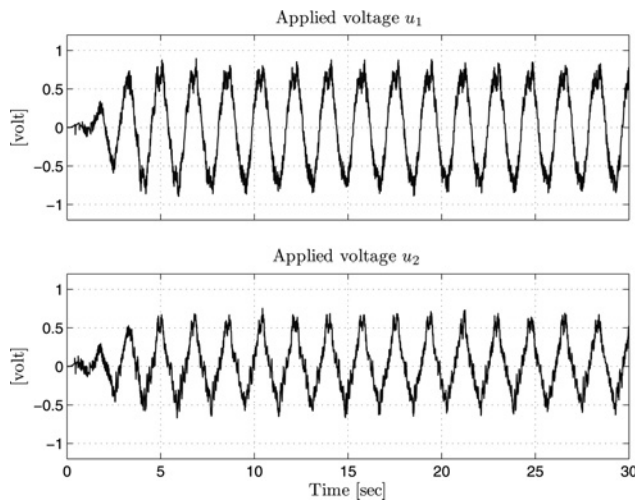


Figure 7 New controller: applied voltages $u_1(t)$ and $u_2(t)$

was used. Finally, to keep a fair comparison scenery, $\sigma = 1$ and matrix Γ_a in (67) were also used.

The results are given in Figs. 6–8, which show the tracking errors $\tilde{q}_1(t)$, $\tilde{q}_2(t)$, the applied control voltage $u_1(t)$, $u_2(t)$ and the estimated parameters $\hat{\theta}_i(t)$, $i = 1, \dots, 8$, respectively.

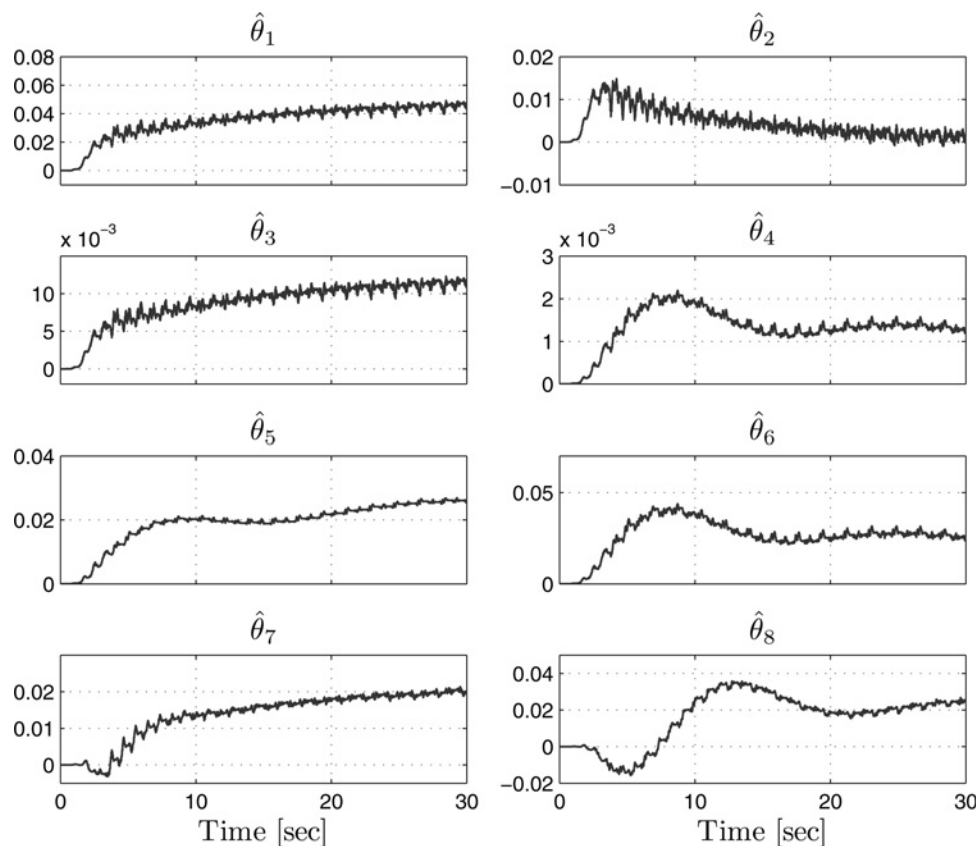


Figure 8 New controller: estimated parameters $\hat{\theta}_i(t)$

See Table 1 for the units of each parameter

4.3 Discussions

Although exponential stability implies that the position error $\tilde{q}(t)$ must tend to zero as time increases, in practice Figs. 3 and 6 reveal the existence of a steady-state oscillatory behaviour. This is due to several factors such as uncompensated Coulomb friction (particularly in joint 2), discrete controller implementation, encoder resolution of 2000 ppr and high-frequency PWM switching of the servo amplifiers.

From a visual examination of Figs. 3 and 6, we have that the ZDQK scheme (58) and the new controller (37) exhibit a settling time of approximately 20.0 s, which is quite reasonable in comparison with other practical implementations of adaptive controllers; see, for example, [1, 7, 8], which show equal or greater settling times than the ones obtained in the present work.

For each joint, the maximum and minimum tracking errors after the settling time were computed. This information is shown in Table 2. The peak tracking errors are smaller in the new controller (37) than in the ZDQK scheme (58). More particularly, the peak-to-peak error in joint 1 is 0.012 rad for the ZDQK scheme, and 0.008 rad for new adaptive controller, which means 33% of improvement. In joint 2, the peak-to-peak error is 0.03 rad

Table 2 Performance of the two controllers: maximum and minimum tracking errors after the settling time

Index, rad	ZDQK	New
$\max_{t \geq 20} \{\tilde{q}_1(t)\}$	0.008	0.004
$\min_{t \geq 20} \{\tilde{q}_1(t)\}$	-0.004	-0.004
$\max_{t \geq 20} \{\tilde{q}_2(t)\}$	0.020	0.010
$\min_{t \geq 20} \{\tilde{q}_2(t)\}$	-0.010	-0.005

for the ZDQK scheme, and 0.0150 rad for the new algorithm, meaning 50% of improvement. Thus, for similar conditions of execution, the new controller behaved better than the ZDQK algorithm.

5 Conclusions

This paper introduced a new control algorithm for the tracking control of a class of robot manipulators. The new algorithm uses only joint position measurements. The class of robot manipulators addressed in this paper assumes DC motors and servo amplifiers in current mode as actuators. Important properties of this class of robot models were discussed and a rigorous stability analysis of the closed-loop system was presented. Our study included experimental evaluations, where the performance of the new controller and a known one was compared. In steady state, the new controller showed better performance in the tracking errors.

6 Acknowledgments

The authors wish to thank the Reviewer for their constructive comments, which helped us to improve the quality of the present paper. This work was supported by Secretaría de Investigación y Posgrado-IPN, CONACyT, and DGEST, Mexico.

7 References

- [1] DALY J.M., SCHWARTZ H.M.: 'Experimental results for output feedback adaptive robot control', *Robotica*, 2006, **24**, pp. 727–738
- [2] ORTEGA R., LORÍA A., SIRA-RAMÍREZ H.H., NICKLASSON P.J.: 'Passivity-based control of Euler–Lagrange systems' (Springer-Verlag, London, 1998)
- [3] DE QUEIROZ M.S., DAWSON D.M., NAGARKATTI S.P., ZHANG F.: 'Lyapunov-based control of mechanical systems' (Birkhäuser, Boston, 2000)
- [4] CANUDAS DE WIT C., SICILIANO B., BASTIN G. (EDS.): 'Theory of robot control' (Springer-Verlag, London, 1996)
- [5] ZHANG F., DAWSON D.M., DE QUEIROZ M.S., DIXON W.E.: 'Global adaptive output feedback tracking control of robot

manipulators'. Proc. 36th IEEE Conf. on Decision and Control, San Diego, CA, 10–12 December 1997, pp. 3634–3639

- [6] ZHANG F., DAWSON D.M., DE QUEIROZ M.S., DIXON W.: 'Global adaptive output feedback tracking control of robot manipulators', *IEEE Trans. Autom. Control*, 2000, **45**, (6), pp. 1203–1208
- [7] ZERGEROGLU E., DAWSON D.M., DE QUEIROZ M.S., KRSTIĆ M.: 'On global output feedback tracking control of robot manipulators'. Proc. IEEE Conf. on Decision and Control, Sydney, Australia, December 2000, pp. 5073–5078
- [8] DIXON W., ZERGEROGLU E., DAWSON D.M., HANNAN M.W.: 'Global adaptive partial state feedback tracking control of rigid-link flexible-joint robots', *Robotica*, 2000, **18**, pp. 325–336
- [9] ARTEAGA M.A.: 'Robot control and parameter estimation with only joint position measurements', *Automatica*, 2003, **39**, pp. 67–73
- [10] ALONGE F., D'IPPOLITO F., RAIMONDI T.: 'A control law for robotic manipulators based on a filtered signal to generate PD action and velocity estimates', *Int. J. Robot. Autom.*, 2007, **22**, (2), pp. 126–138
- [11] SCIAVICCO L., SICILIANO B.: 'Modelling and control of robot manipulators' (Springer, London, 2000)
- [12] KELLY R., SANTIBÁÑEZ V., LORIA A.: 'Control of robot manipulators in joint space' (Springer-Verlag, London, 2005)
- [13] CHAN S.P.: 'An efficient algorithm for identification of robot parameters including drive characteristics', *J. Intell. Robot. Syst.*, 2001, **32**, (3), pp. 291–305
- [14] ARIMOTO S.: 'Fundamental problems of robot control: part 1, innovations in the realm of robot servo-loops', *Robotica*, 1995, **13**, pp. 19–27
- [15] ARIMOTO S.: 'Fundamental problems of robot control: part 2, a nonlinear circuit theory towards an understanding of dexterous motions', *Robotica*, 1995, **13**, pp. 111–122
- [16] HORN R.A., JOHNSON C.R.: 'Matrix analysis' (Cambridge University Press, Cambridge, 1985)
- [17] KRSTIĆ M., KANELAKOPOULOS I., KOKOTOVIĆ P.: 'Nonlinear and adaptive controller control design' (John Wiley and Sons, New York, 1995)
- [18] KHALIL H.: 'Nonlinear systems' (Prentice-Hall, Upper Saddle River, 2002, 3rd edn.)
- [19] SANTIBÁÑEZ V., KELLY R.: 'Global asymptotic stability of bounded output feedback tracking control for robot manipulators'. 40th IEEE Conf. on Decision and Control, Orlando, FL, December 2001, pp. 1378–1379

[20] NUNES E.V.L., HSU L.: 'Global tracking for robot manipulators using a simple causal PD controller plus feedforward', *Robotica*, 2010, **28**, (1), pp. 23–34

[21] AGUIÑAGA-RUIZ E., ZAVALA-RÍO A., SANTIBÁÑEZ V., REYES F.: 'Global trajectory tracking through static feedback for robot manipulators with bounded inputs', *IEEE Trans. Control Syst. Technol.*, 2009, **17**, (4), pp. 934–944

[22] LORIA A., KELLY R., TEELA.: 'Uniform parametric convergence in the adaptive control of mechanical systems', *Eur. J. Control*, 2005, **11**, (2), pp. 87–100, available at: ftp://ftp.lss.supelec.fr/pub/users/loria/aloria_publicis/ejc-robots.pdf

[23] LJUNG L.: 'System identification: theory for the user' (Prentice-Hall, Englewood Cliffs, NJ, 1999, 2nd edn.)

8 Appendix 1: hyperbolic functions

The tangent hyperbolic function is defined as

$$\tanh(x) = \frac{e^x - e^{-x}}{e^x + e^{-x}}$$

where $x \in \mathbb{R}$. The tangent hyperbolic function can be arranged in a vector in the following way

$$\tanh(z) = [\tanh(z_1), \dots, \tanh(z_n)]^T$$

and the following properties are accomplished by $\tanh(z)$:

(a) The Euclidean norm of $\tanh(z)$ satisfies

$$\|\tanh(z)\| \leq \begin{cases} \|z\| & \forall z \in \mathbb{R}^n \\ \sqrt{n} & \forall z \in \mathbb{R}^n \end{cases}$$

(b) The time derivative of $\tanh(z)$ is given by

$$\frac{d}{dt} \tanh(z) = \text{Sech}^2(z) \dot{z}$$

where $\text{Sech}^2(z) = \text{diag}\{\text{sech}^2(z_1), \dots, \text{sech}^2(z_n)\}$ and

$$\text{sech}(x) = \frac{2}{e^x + e^{-x}} = \frac{1}{\cosh(x)}$$

(c) The maximum eigenvalue of the matrix $\text{Sech}^2(x)$ is one for all $x \in \mathbb{R}^n$, that is

$$\lambda_{\max}\{\text{Sech}^2(x)\} = 1, \quad \forall x \in \mathbb{R}^n$$

On the other hand, the time derivative of $\ln(\cosh(x))$, $x \in \mathbb{R}$, is given by

$$\frac{d}{dt} \ln(\cosh(x)) = \tanh(x) \dot{x}$$

Thus, the property

$$\sqrt{\sum_{i=1}^n \ln(\cosh(z_i))} \geq \frac{1}{\sqrt{2}} \|\tanh(z)\| \forall z = [z_1 \dots z_n]^T \quad (68)$$

holds.

9 Appendix 2: local stability of the reduced dynamics (48)

This appendix is devoted to show the local uniform stability of the reduced dynamics (48), obtained in the proof of Proposition 2, and to derive the inequality (51).

By using Assumption 1 in (8) and (9), the robot model property (12), and property (68), a lower bound on $V(t, \tilde{q}, \dot{\tilde{q}}, \tilde{\theta})$ in (50) is given by

$$V(t, \tilde{q}, \dot{\tilde{q}}, \tilde{\theta}) \geq \eta^T P \eta + \frac{1}{2} \tilde{\theta}^T \Gamma_a^{-1} \tilde{\theta}$$

where the vector $\eta \in \mathbb{R}^n$ was defined in (39) and

$$P = \begin{bmatrix} \sigma^{-1} \lambda_{\min}\{K_p\} & -\frac{\epsilon_2}{2} \sqrt{2} \lambda_{\max}\{\overline{M}^*(q)\} \\ -\frac{\epsilon_2}{2} \sqrt{2} \lambda_{\max}\{\overline{M}^*(q)\} & \frac{1}{2} \lambda_{\min}\{\overline{M}^*(q)\} \end{bmatrix}$$

with matrix $\overline{M}^*(q)$ defined in (9). The sufficient and necessary condition for P to be positive definite is

$$0 < \epsilon_2 < \frac{\sqrt{\sigma^{-1} \lambda_{\min}\{K_p\} \lambda_{\min}\{\overline{M}^*(q)\}}}{\lambda_{\max}\{\overline{M}^*(q)\}}$$

which shows that with large numerical gain of the proportional gain K_p the function $V(t, \tilde{q}, \dot{\tilde{q}}, \tilde{\theta})$ in (50) is globally positive definite and decrescent.

The time-derivative of the Lyapunov function candidate $V(t, \tilde{q}, \dot{\tilde{q}}, \tilde{\theta})$ in (50) along the slow dynamics (48) is given by

$$\begin{aligned} \dot{V}(t, \tilde{q}, \dot{\tilde{q}}, \tilde{\theta}) &= \frac{1}{2} \dot{\tilde{q}}^T [\overline{C}(q, \dot{q}) - \overline{C}^*(q, \dot{q})]^T \dot{\tilde{q}} - \dot{\tilde{q}}^T [\overline{F}_v + K_v] \dot{\tilde{q}} \\ &\quad - \dot{\tilde{q}}^T \overline{h}(\tilde{q}, \dot{\tilde{q}}) + \epsilon_2 \tanh(\sigma \tilde{q})^T \overline{C}^*(q, \dot{q})^T \dot{\tilde{q}} \\ &\quad + \epsilon_2 \sigma \dot{\tilde{q}}^T \text{Sech}^2(\sigma \tilde{q}) \overline{M}^*(q) \dot{\tilde{q}} + \epsilon_2 \tanh(\sigma \tilde{q})^T \\ &\quad \times [-\overline{F}_v + K_v] \dot{\tilde{q}} - K_p \tanh(\sigma \tilde{q}) - \overline{h}(\tilde{q}, \dot{\tilde{q}}) \end{aligned} \quad (69)$$

which was obtained by taking into account the robot model property in (13). The next step is to find a proper upper

bound in each term of (69)

$$\begin{aligned}
 \frac{1}{2} \dot{\tilde{q}}^T [\bar{C}(q, \dot{q}) - \bar{C}^*(q, \dot{q})]^T \dot{\tilde{q}} &\leq k_{C1} \|\dot{\tilde{q}}\|^3 + k_{C1} \mu_1 \|\dot{\tilde{q}}\|^2 \\
 -\dot{\tilde{q}}^T [\bar{F}_v + K_v] \dot{\tilde{q}} &\leq -\lambda_{\min}\{\bar{F}_v + K_v\} \|\dot{\tilde{q}}\|^2 \\
 -\dot{\tilde{q}}^T \bar{b}(\tilde{q}, \dot{\tilde{q}}) &\leq k_{C1} \mu_1 \|\dot{\tilde{q}}\|^2 + \gamma_1 \|\tanh(\sigma \tilde{q})\| \|\dot{\tilde{q}}\| \\
 \epsilon_2 \tanh(\sigma \tilde{q})^T \bar{C}^*(q, \dot{q})^T \dot{\tilde{q}} &\leq \epsilon_2 k_{C1} \sqrt{n} \|\dot{\tilde{q}}\|^2 \\
 &\quad + \epsilon_2 k_{C1} \mu_1 \|\tanh(\sigma \tilde{q})\| \|\dot{\tilde{q}}\| \\
 \epsilon_2 \sigma \dot{\tilde{q}}^T \text{Sech}^2(\sigma \tilde{q}) \bar{M}(q) \dot{\tilde{q}} &\leq \epsilon_2 \sigma \|\bar{M}(q)\| \|\dot{\tilde{q}}\|^2 \\
 -\epsilon_2 \tanh(\sigma \tilde{q}) [\bar{F}_v + K_v] \dot{\tilde{q}} &\leq \epsilon_2 \lambda_{\text{Max}}\{\bar{F}_v + K_v\} \\
 &\quad \times \|\tanh(\sigma \tilde{q})\| \|\dot{\tilde{q}}\| \\
 -\epsilon_2 \tanh(\sigma \tilde{q})^T K_p \tanh(\sigma \tilde{q}) &\leq -\epsilon_2 \lambda_{\min}\{K_p\} \|\tanh(\sigma \tilde{q})\|^2 \\
 -\epsilon_2 \tanh(\sigma \tilde{q})^T \bar{b}(\tilde{q}, \dot{\tilde{q}}) &\leq \epsilon_2 k_{C1} \mu_1 \|\tanh(\sigma \tilde{q})\| \|\dot{\tilde{q}}\| \\
 &\quad + \epsilon_2 \gamma_1 \|\tanh(\sigma \tilde{q})\|^2
 \end{aligned} \tag{70}$$

where γ_1 is defined in (34). The bounds in (70) were obtained by using the inequality (16), Property 3 of the residual dynamics $\bar{b}(\tilde{q}, \dot{\tilde{q}})$, the inequality $\|\dot{\tilde{q}}\| \leq \mu_1 + \|\dot{\tilde{q}}\|$,

and properties of the hyperbolic functions in Appendix 1. Now, by using the inequalities in (70) we are able to write an upper bound on $\dot{V}(t, \tilde{q}, \dot{\tilde{q}}, \ddot{\tilde{q}})$ as follows:

$$\begin{aligned}
 \dot{V}(t, \tilde{q}, \dot{\tilde{q}}, \ddot{\tilde{q}}) &\leq -U(\tilde{q}, \dot{\tilde{q}}) \\
 &= - \begin{bmatrix} \|\tanh(\sigma \tilde{q})\| \\ \|\dot{\tilde{q}}\| \end{bmatrix}^T Q \begin{bmatrix} \|\tanh(\sigma \tilde{q})\| \\ \|\dot{\tilde{q}}\| \end{bmatrix} \tag{71}
 \end{aligned}$$

where (see equation at the bottom of the page)

where γ_1 , γ_2 and γ_3 are given in (34), (35) and (36), respectively. Let us define the set

$$D = \{x \in \mathbb{R}^{2n+r} : \|x\| \leq d\} \tag{72}$$

with $x = [\tilde{q}^T \ \dot{\tilde{q}}^T \ \ddot{\tilde{q}}^T]^T$. Then, for all $x \in D$ and fixed $\epsilon_2 > 0$ there are large enough gain matrices K_p and K_v such that the matrix Q is diagonal dominant and positive definite. Summarising, these are the conditions to assure that the state-space origin of the reduced system (48) is uniformly stable in the Lyapunov sense [18].

Finally, the function $U(\tilde{q}, \dot{\tilde{q}})$ in (51) needed in the proof of Proposition 2 is obtained from (71).

$$Q = \begin{bmatrix} \epsilon_2 [\lambda_{\min}\{K_p\} - \gamma_1] & -\frac{1}{2} \gamma_1 - \epsilon_2 \frac{1}{2} [\gamma_2 + \lambda_{\text{Max}}\{K_v\}] \\ -\frac{1}{2} \gamma_1 - \epsilon_2 \frac{1}{2} [\gamma_2 + \lambda_{\text{Max}}\{K_v\}] & \lambda_{\min}\{\bar{F}_v + K_v\} - 2k_{C1} \mu_1 - \epsilon_2 \gamma_3 - k_{C1} \|\dot{\tilde{q}}\| \end{bmatrix}$$